Cell Research (2010) 20:688-700.

www.nature.com/cr

ORIGINAL ARTICLE

Disruption of the 1-deoxy-D-xylulose-5-phosphate reductoisomerase (*DXR*) gene results in albino, dwarf and defects in trichome initiation and stomata closure in *Arabidopsis*

Shufan Xing[1], Jin Miao[1], Shuang Li[1], Genji Qin[1], Si Tang[1], Haoni Li[1], Hongya Gu[1, 2], Li-Jia Qu[1, 2]

[1]*National Laboratory for Protein Engineering and Plant Genetic Engineering, College of Life Sciences, Peking University, Beijing 100871, China;* [2]*The National Plant Gene Research Center (Beijing), Beijing 100101, China*

1-Deoxy-D-xylulose-5-phosphate reductoisomerase (DXR) is an important enzyme involved in the 2-C-methyl-D-erythritol-4-phosphate (MEP) pathway which provides the basic five-carbon units for isoprenoid biosynthesis. To investigate the role of the MEP pathway in plant development and metabolism, we carried out detailed analyses on a *dxr* mutant (GK_215C01) and two *DXR* transgenic co-suppression lines, OX-DXR-L2 and OX-DXR-L7. We found that the *dxr* mutant was albino and dwarf. It never bolted, had significantly reduced number of trichomes and most of the stomata could not close normally in the leaves. The two co-suppression lines produced more yellow inflorescences and albino sepals with no trichomes. The transcription levels of genes involved in trichome initiation were found to be strongly affected, including *GLABRA1*, *TRANSPARENT TESTA GLABROUS 1*, *TRIPTYCHON* and *SPINDLY*, expression of which is regulated by gibberellic acids (GAs). Exogenous application of GA_3 could partially rescue the dwarf phenotype and the trichome initiation of *dxr*, whereas exogenous application of abscisic acid (ABA) could rescue the stomata closure defect, suggesting that lower levels of both GA and ABA contribute to the phenotype in the *dxr* mutants. We further found that genes involved in the biosynthetic pathways of GA and ABA were coordinately regulated. These results indicate that disruption of the plastidial MEP pathway leads to biosynthetic deficiency of photosynthetic pigments, GAs and ABA, and thus the developmental abnormalities, and that the flux from the cytoplasmic mevalonate pathway is not sufficient to rescue the deficiency caused by the blockage of the plastidial MEP pathway. These results reveal a critical role for the MEP biosynthetic pathway in controlling the biosynthesis of isoprenoids.

Keywords**:** MEP pathway, *DXR*, trichome development, stomata closure, GA, ABA
Cell Research (2010) **20**:688-700. doi:10.1038/cr.2010.54; pulished online 20 April 2010

Introduction

Isoprenoids are the most functionally and structurally varied metabolites in plants, with tens of thousands of compounds reported to date [1, 2]. They play a critical role in plant respiration, photosynthesis, regulation of growth and development. They also act to protect plants against herbivores and pathogens, to attract pollinators and seed-dispersing animals, and to influence competition among plant species [2]. All natural isoprenoids are derived from two basic five-carbon molecules, isopentenyl diphosphate (IPP) and its allylic isomer dimethylallyl diphosphate (DMAPP) [1, 3]. In higher plants, the isoprenoid building units are formed from two pathways that operate in different subcellular compartments [4-6]. One is the mevalonate (MVA) pathway, which is localized in the cytosol [7]. The other is the 2-C-methyl-D-erythritol-4-phosphate (MEP) pathway, which is localized in plastids [7]. Sesquiterpenes, triterpenes, cytokinins and brassinosteroids are synthesized via the MVA

Correspondence: Li-Jia Qu
Fax: +86-10-6275-1841
E-mail: qulj@pku.edu.cn
Received 14 October 2009; revised 15 December 2009; accepted 26 January 2010; published online 20 April 2010

pathway, while carotenoids, lutein, chlorophyll side chains, ubiquinone, gibberellic acids (GAs) and abscisic acid (ABA) are synthesized via the MEP pathway (Figure 1, [7-9]).

The MVA pathway has been extensively studied since its discovery in the 1950s, and has been reviewed in detail [1, 3]. Different from the MVA pathway, the MEP pathway was first identified in bacteria about 15 years ago and later in plants [6, 10]. Currently, all the enzymes involved in the MEP pathway have been identified. In the first step of this pathway, 1-deoxy-D-xylulose-5-phosphate synthase (DXS) catalyzes the formation of 1-deoxy-D-xylulose-5-phosphate (DXP) from pyruvate and D-glyceraldehyde-3-phosphate [11-13]. Then, DXP is transformed to MEP, catalyzed by DXR [14]. Finally, MEP is converted to IPP and DMAPP after consecutive steps catalyzed by 2-C-methyl-D-erythritol-4-phosphate cytidylyltransferase (CMS), 4-(cytidine 5′-diphospho)-2-C-methyl-D-erythritol kinase (CMK), 2-C-methyl-D-erythritol-2,4-cyclodiphosphate synthase (MCS), 4-hydroxy-3-methylbut-2-enyl diphosphate synthase (HDS), 4-hydroxy-3-methylbut-2-enyl diphosphate reductase (HDR) and isopentenyl diphosphate isomerase (IPI) [9, 5, 15, 16].

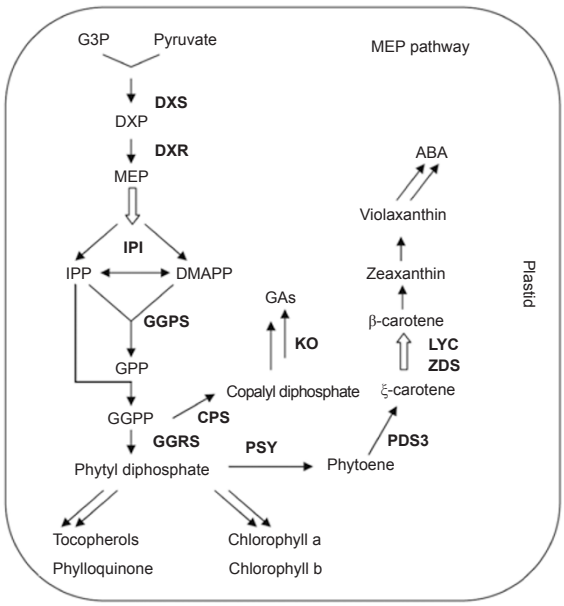

Figure 1 MEP pathway with plastids localization in plants (modified from Qin *et al*. [30]). The symbol for anabolic reactions is a solid arrow. Open arrows and double solid arrows depict multiple enzymatic steps. Certain key enzymes are written in bold. G3P: glycerol triphosphate; DXP: 1-deoxy-D-xylulose-5-phosphate; MEP: 2-C-methyl-D-erythritol-4-phosphate; IPP: isopentenyl diphosphate; DMAPP: dimethylallyl diphosphate; GPP: geranyl diphosphate; GGPP: geranyl geranyl diphosphate; DXS: 1-deoxy-D-xylulose-5-phosphate synthase; DXR: 1-deoxy-D-xylulose-5-phosphate reductoisomerase; IPI: isopentenyl diphosphate; GGPS: geranylgeranyl diphosphate synthase; GGRS: geranylgeranyl reductase; PSY: phytoene synthase; PDS: phytoene desaturase; ZDS: ξ-carotene desaturase; LYC: lycopene cyclase; CPS: copalyl diphosphate synthase; KO: ent-kaurene oxidase.

In the MEP pathway, MEP serves as the precursor not only for IPP or DMAPP, but also for vitamin B1 [17, 18]. Previous studies have shown that DXR played a critical role in directing the intermediate flux into IPP and DMAPP biosynthetic pathways [19, 20]. Overexpression of *DXR* resulted in an increase in biosynthesis of essential oils in mint and an increase in photosynthetic pigment levels in *Arabidopsis* [20, 21]. All results suggest that DXR contributes more specifically to the MEP pathway than DXS. The *Arabidopsis* genome contains only one *DXR* gene. The transcript pattern of *DXR* covers almost all plant organs, with the highest level in inflorescence tissue [19, 22]. Blocking of DXR activity using the specific inhibitor fosmidomycin (FSM) led to the accumulation of DXR protein, the bleach phenotype, and the failure of seedling establishment [19, 20, 23-26]. An insertion mutant of *DXR* was found to be an albino, and down-regulation of *DXR* transcript level resulted in abnormal chloroplast development [20, 27]. However, until now, the phenotypic analysis was only restricted to chloroplast development and photosynthetic pigment biosynthesis.

In addition to the photosynthetic pigments, both GAs and ABA are important chemical molecules synthesized from the plastidial geranyl geranyl diphosphate (GGPP) precursor, which is derived from IPP and DMAPP of the MEP pathway [8, 9, 28, 29]. The biosynthetic pathways for GA and ABA have been well documented [7]. However, how the MEP pathway contributes to the biosynthesis of GA and ABA remains ambiguous, due to the complexity of IPP and DMAPP biosynthesis [7, 25]. Potential crosstalk of IPP and DMAPP between the MVA and MEP pathways might affect the downstream biosynthesis, and channeling of the IPP and DMAPP precursors to different isoprenoid biosynthetic pathway branches is tightly controlled. Previous studies indicated that the amount of ent-kaurene, the important precursor for GA biosynthesis, was decreased in plants with reduced DXR activity [25]. Exogenous application of GAs to the medium could partially rescue the dwarf phenotype of the *pds3* mutant [30]. Other research indicated that levels of not only GAs but also other important compounds were decreased as a result of the metabolic disruption in the mutants of enzymes involved in the MEP pathway [21, 30-34]. However, no detailed analyses have been

reported about the developmental and the physiological changes due to the complete blockage of the MEP pathway.

In order to investigate the contribution of the MEP pathway to the developmental and physiological processes in *Arabidopsis*, we characterized a *dxr* mutant and two *DXR* transgenic co-suppression lines in this study. The transcript changes of selected enzymes involved in the isoprenoid biosynthetic pathway were analyzed to investigate the flux regulation mechanism of plastid isoprenoid biosynthesis.

Results

Phenotypic analysis to the DXR null mutant

In order to understand the effects of the MEP pathway

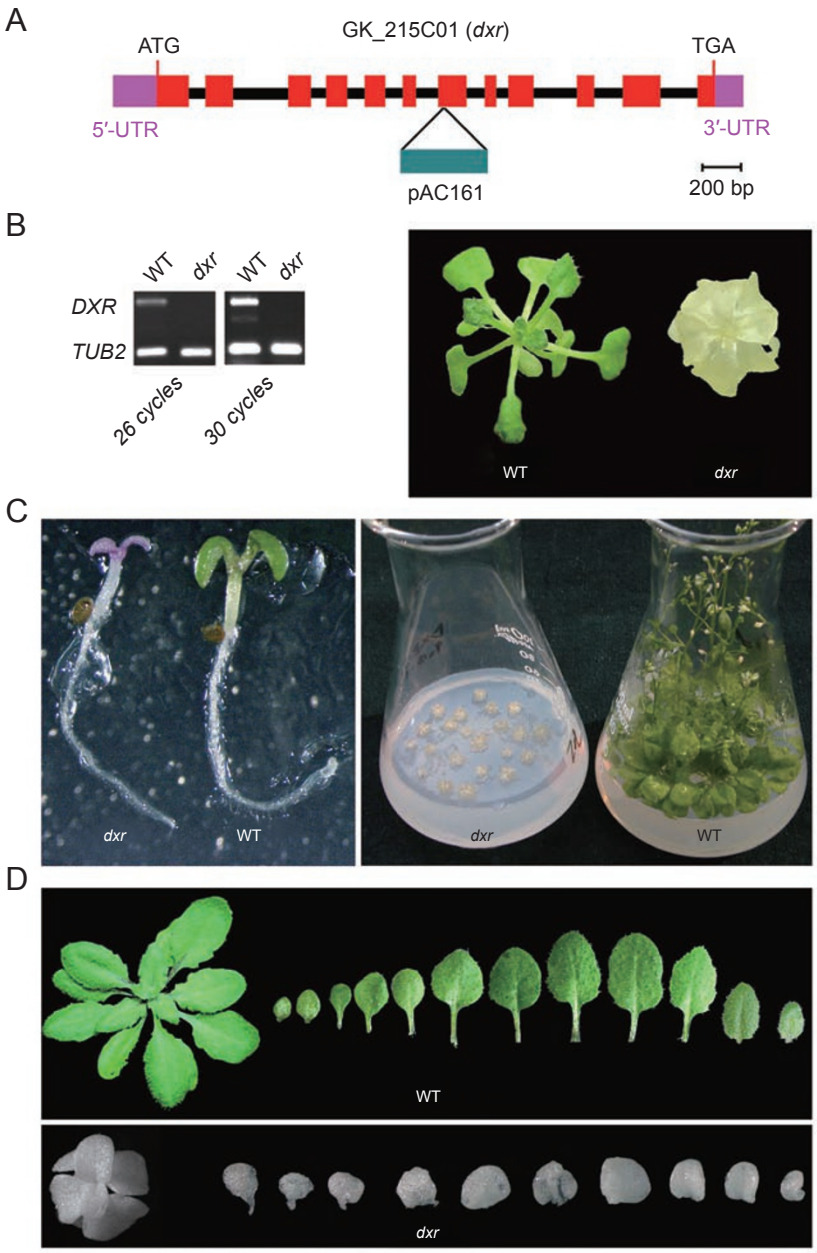

Figure 2 Identification of *DXR* null mutant. **(A)** *DXR* gene structure and the T-DNA insertion site in GK-215C01 mutant. **(B)** RT-PCR analysis for the transcription level of *DXR* gene in wild-type (WT) plants and GK-215C01 mutant plants. **(C)** *dxr* seedling with purple cotyledons; adult *dxr* mutant plants and WT plants grown on MS medium for 2 months. **(D)** 40-day WT plants with 12 leaves and 60-day homozygous *dxr* mutant with 10 leaves.

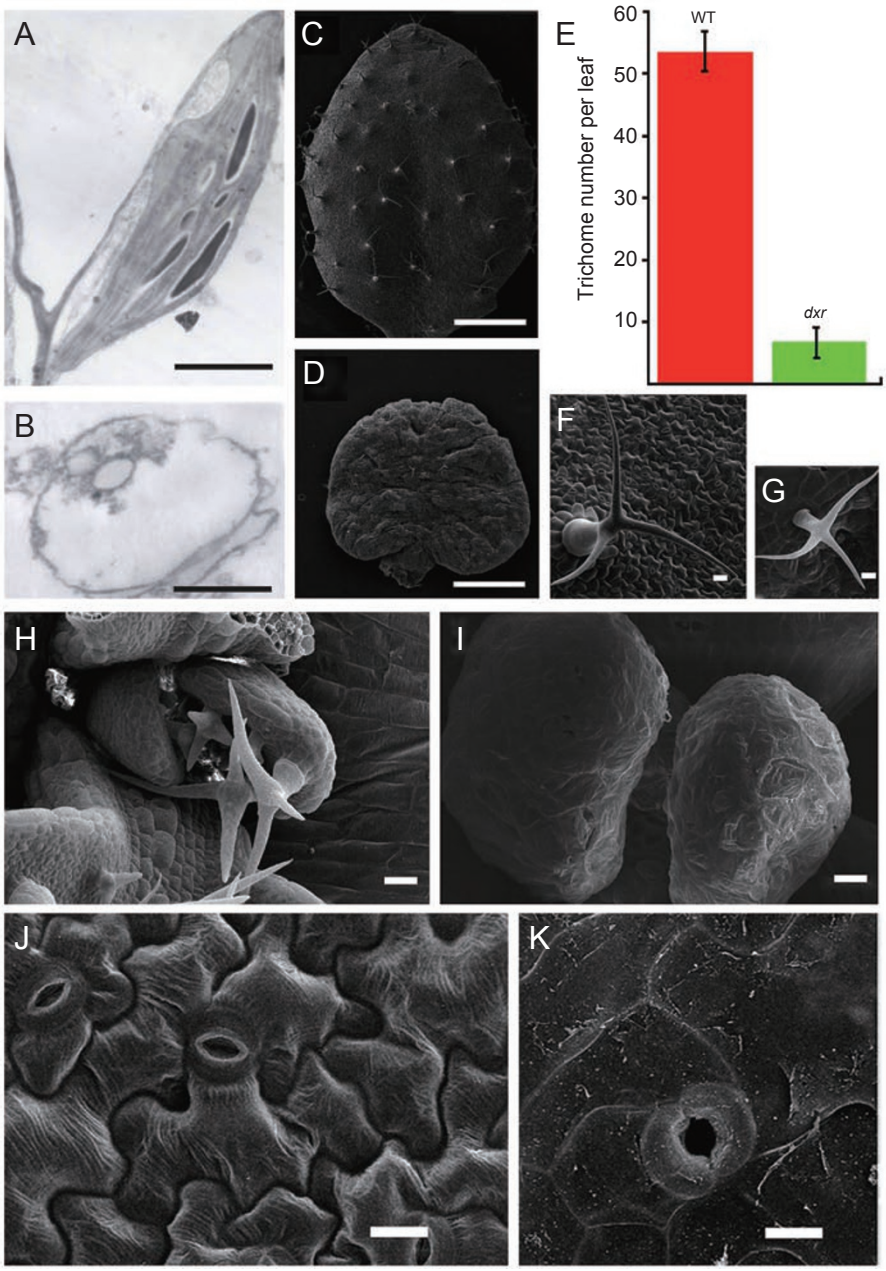

Figure 3 Detailed phenotypes of wild-type (WT) plants **(A**, **C**, **F**, **H**, **J)** and *dxr* null mutants **(B**, **D**, **G**, **I**, **K)**. **(A**, **B)** The development of plastids in WT and *dxr* mutant plants, bar = 2.2 μm. **(C**-**E)** The statistical analyses of trichome number on four leaves of WT and *dxr* mutant, WT: 53 ± 3.7 ($n \geq 10$), *dxr*: 6.2 ± 2.4 ($n \geq 10$); in **(C**, **D)**, bar = 1 cm. **(C**, **F**, **H)** The trichome development of WT *Arabidopsis* plant. **(D**, **G**, **I)** The trichome development of *dxr* null mutant. In **(F**, **G)**, bar = 200 μm; in **(H**, **I)**, bar = 300 μm. **(J**, **K)** The stomata of WT and *dxr* mutant plants, bar = 100 μm.

on plant development, we obtained a T-DNA insertion mutant line, GK-215C01 [35]. The T-DNA insertion site of GK-215C01 is localized in the seventh exon of the *DXR* gene (Figure 2A). RT-PCR analysis showed that the expression of *DXR* was abolished (Figure 2B), indicating that GK-215C01 is a null mutant, and it was thus renamed as *dxr*. Phenotypic analysis of *dxr* shows that *dxr* has deficiencies in multiple developmental and physiological processes. The homozygous *dxr* mutants display an albino phenotype and grow purple cotyledons (Figure 2C). They grow round and small true leaves with very short petioles, and never bolt during their whole lifetime (Figure 2C). The growth of *dxr* mutants is severely retarded, since the 60-day-old *dxr* mutant plants have

only 10 leaves, whereas the 40-day-old wild-type plants have as many as 12 leaves and begin to bolt (Figure 2D). Because the homozygous *dxr* mutants could not produce offspring, we could only obtain the homozygous *dxr* mutants from the normally growing *dxr* heterozygous mutant. When the homozygous mutant was transferred to the soil, it lost water almost immediately and wilted to death (data not shown). For further observations, the *dxr* plants had to be grown on MS plates with 1% sucrose (Figure 2C).

To investigate the fine cellular structure changes of the *dxr* mutant, we performed scanning electron microscope (SEM) and transmission electron microscope (TEM) analyses. The TEM results showed that, while the wild-type (WT) plants developed normal chloroplasts (Figure 3A), the *dxr* mutant only developed proplastids, with no normal thylakoids observed (Figure 3B), suggesting that the plastid development was blocked at the pro-plastid stage. The SEM results showed that, compared to the WT (Figure 3C, 3F and 3H), not only did *dxr* mutants grow reduced numbers of trichomes (Figure 3D, 3E and 3I) but also their trichomes were smaller than those of WT plants, although the trichome shapes were similar (Figure 3G). An interesting phenomenon of the *dxr* mutant is that the latest grown leaves are usually glabrous (Figure 3I). Besides the trichome developmental phenotype, we also found that, compared with the WT (Figure 3J), the stomata of the *dxr* mutant had a larger opening (Figure 3K), indicating that the *dxr* stomata closed abnormally.

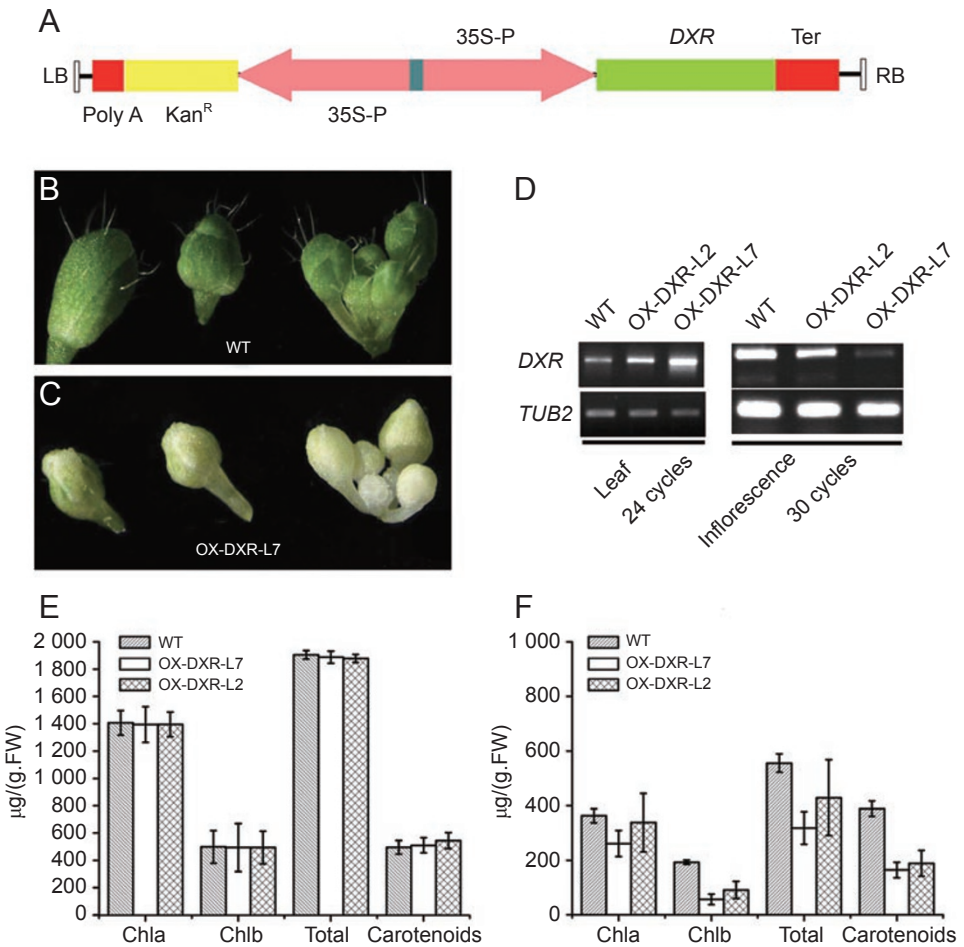

Figure 4 Photosynthetic pigments level in *DXR* co-suppressed inflorescence. **(A)** Structure of the construct to over-express *DXR* in *Arabidopsis* plants. **(B)** Green inflorescence and flower buds from WT plants. **(C)** Albino inflorescence and flower buds from OX-DXR-L7 plants. **(D)** Co-suppressed *DXR* transcript level in OX-DXR-L2 and OX-DXR-L7 plants, in comparison with WT plants. **(E)** Photosynthetic pigments level of green leaves from WT, OX-DXR-L2, and OX-DXR-L7 plants. **(F)** Photosynthetic pigments level of inflorescence from WT, OX-DXR-L2, and OX-DXR-L7 plants. In **(E**, **F)**, values represent means and standard deviations from populations of at least 20 individuals in three independent biological repeats.

Over-expression of DXR in Arabidopsis led to transgene-induced gene silencing

We constructed an over-expression vector for the *DXR* gene (Figure 4A). Attempts to create *DXR* over-expression lines in *Arabidopsis* resulted in some transformants growing pale green or albino inflorescences (Figure 4B and 4C, and Supplementary information, Figure S1). These tissue-specific pale green or albino phenotypes were stably and regularly inherited in two lines, OX-DXR-L2 and OX-DXR-L7. In order to investigate whether this stable phenotype was related to transgene-induced gene silencing, the *DXR* transcript level was analyzed in green leaves and pale green or albino inflorescences from either OX-DXR-L2 or OX-DXR-L7, respectively. The results showed that *DXR* expression is up-regulated in green leaves, but down-regulated in the gray or albino inflorescences of the same plant (Figure 4D). A much more severe decrease of the *DXR* transcript level was detected in the albino inflorescences of OX-DXR-L7 plants than in those of OX-DXR-L2 plants (Figure 4D). Accordingly, the contents of photosynthetic pigments were also measured in different tissues of both OX-DXR-L2 and OX-DXR-L7 lines. In OX-DXR-L2 inflorescences, chlorophyll a (Chl a) was reduced to 93.2% of the WT level. The levels of chlorophyll b (Chl b) and carotenoids decreased to 47.3% and 48.5% of the WT levels, respectively (Figure 4F). In OX-DXR-L7 inflorescences, the levels of Chl a, Chl b and carotenoids were reduced to 72%, 29.5% and 42.3% of the corresponding WT levels, respectively (Figure 4F). However, in leaves with increased levels of DXR the contents of photosynthetic pigments did not change much (Figure 4E), suggesting that the metabolic balance was more sensitive to a reduction in the *DXR* transcript level than an increase.

As the *dxr* mutant did not develop flowers, the *DXR* co-suppression inflorescences provided an excellent model to analyze the effect of the MEP pathway on the flower development process. Consistent with the observation from the *dxr* leaves, OX-DXR-L7 also showed a phenotype of reduced trichome number on the sepal of the albino flower (Figure 4C). The albino flower buds were smaller and displayed difficulty in opening (Supplementary information, Figure S1).

DXR transcript level affects the transcription of many genes involved in carotenoid, chlorophyll, GA and ABA biosynthesis pathways

In many cases, the changed expression levels of enzymes induce complicated metabolic changes, which consequently result in multiple developmental or physiological deficiencies in plants. Previous research has shown that mutants of enzymes involved in the MEP pathway always show feedback regulation [30, 32]. It was thus reasonable to hypothesize that the same kind of metabolic changes might exist in the *dxr* mutant or tissues with reduced *DXR* expression levels.

To investigate this possibility, 10 genes, i.e., *DXS*, *GGPS*, *GGRS*, *IPI*, *GA3*, *PDS1*, *PDS3*, *ZDS*, *LYC* and *PSY*, were chosen [7], and their transcript levels were examined. DXS catalyzes the first committed step of the MEP pathway (Figure 1). DXS and DXR are both shown to be related to flux regulation in the MEP pathway. GGRS, GGPS and IPI are enzymes acting at the steps close to the branching points of the MEP pathway (Figure 1). GA3 is shown to be involved in GA_3 biosynthesis. PDS, ZDS and LYC regulate the biosynthesis of all kinds of carotenoids (Figure 1). Some of those carotenoids can be converted into ABA (Figure 1). In *DXR* over-expressed leaf tissue, many of the genes examined showed an increase in transcript level. The *PDS3* gene had the highest increase to about 2.2 times that of the WT level (Figure 5). However, in gene-silenced albino flower tissues, the transcript level of all these genes decreased. The transcript level of *GGPS* was most significantly reduced, to about 19.1% of the WT level (Figure 5). Notably, there was an obvious decrease in GA3 transcript level, suggesting that the biosynthesis of GA was reduced (Figure 5). ABA biosynthesis might also be reduced due to the decrease in the transcript levels of genes involved in carotenoid biosynthesis (Figure 5). The above data indi-

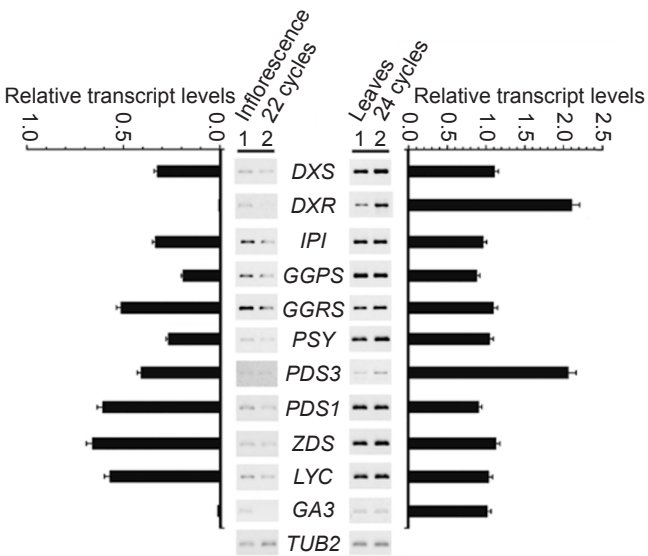

Figure 5 Expression analyses of genes involved in MEP and related biosynthetic pathways in inflorescence and leaves. 1, WT plants; 2, OX-DXR-L7 transgenic plants. The relative transcript level is calculated from three independent experiments.

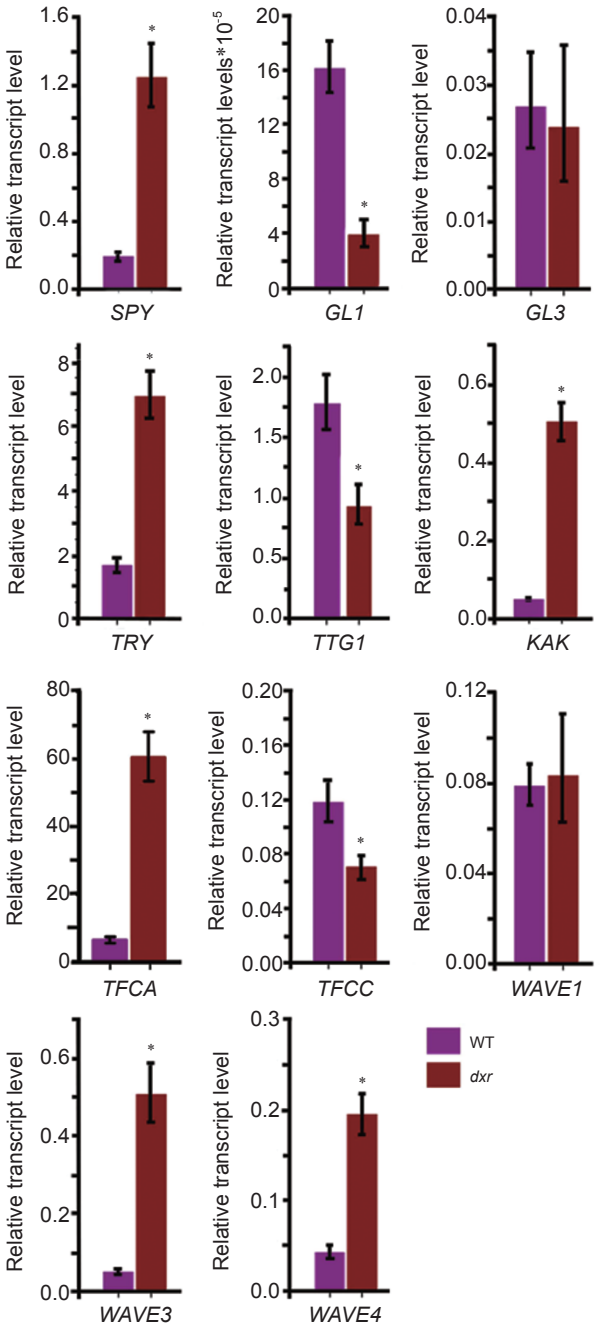

Figure 6 Expression analyses of regulators for trichome development. Values represent means and standard deviations from at least two independent experiments (only one representative one is shown here), each with three biological replicates. Asterisk marks the gene with significant change at the transcription level.

cate that the MEP pathway and downstream metabolic pathways are coordinately regulated through the regulation of the expression levels of key enzymes involved.

Trichome defects in dxr might result from abnormal GA-regulated initiation and endo-reduplication

Trichomes develop in four steps: initiation, endo-reduplication, branching and expansion [36-42]. To assess the developmental deficiencies of trichome in *dxr*, we examined the expression of the regulators involved in different steps of trichome development. These regulators include *GLABRA1* (*GL1*), *GL3*, *TRIPTYCHON* (*TRY*), *TRANSPARENT TESTA GLABROUS 1* (*TTG1*), *SPINDLY* (*SPY*), *TUBULIN FOLDING FACTOR A* (*TFCA*), *TUBULIN FOLDING FACTOR C* (*TFCC*), *KAKTUS* (*KAK*), *WASP family Verprolin-homologous protein 1* (*WAVE1*), *WAVE3*, and *WAVE4*. GL1, GL3, GL2, and TTG1 are known as positive regulators of trichome initiation, while TRY acts as an important negative regulator in this step. Both SPY and KAK are involved in negative regulation of trichome endo-reduplication. TFCA and TFCC are positive regulators of the trichome branching step. WAVE1, WAVE3, and WAVE4 can positively regulate the final trichome expansion step.

Our quantitative real-time PCR results revealed obvious expression changes of several important genes in the *dxr* mutant (Figure 6). The positive regulators of trichome initiation such as *GL1* and *TTG1* had an obvi-

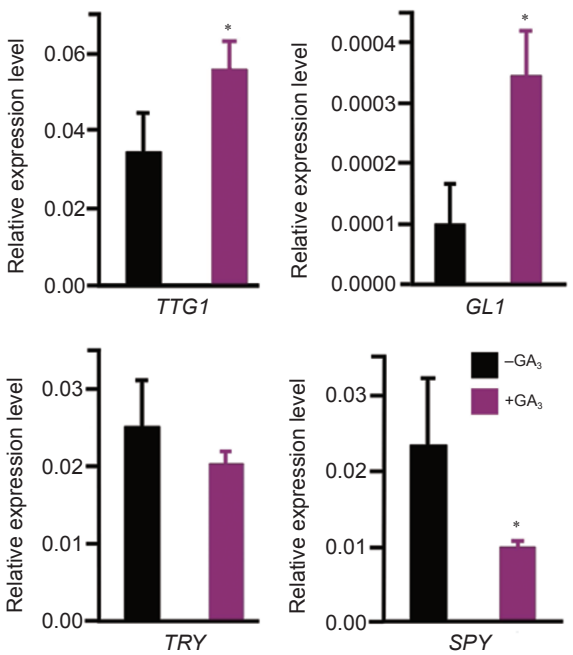

Figure 7 Expression analyses of regulators for trichome development in plants with or without GA_3 treatment. Values represent means and standard deviations from at least two independent experiments (only one representative one is shown here), each with three biological replicates. Asterisk marks the gene with significant change at the transcription level.

ous decrease in their transcript levels, and the expression level of the negative regulator *TRY* was highly increased, consistent with the observed phenotype of reduced trichome initiation. Both *SPY* and *KAK* had an increase in their expression levels, suggesting a potential defect in trichome endo-reduplication. Notably, most of these genes were strongly regulated by GA_3. When 10 μM GA_3 was applied, the transcript levels of *GL1*, *TTG1*, and *SPY* significantly increased or decreased, in a tendency opposite to that in *dxr* mutant (Figure 7). This result is consistent with the important role of GAs in trichome formation and development [43-45].

Exogenous application of GA_3 could partially rescue trichome initiation in dxr mutant

In order to further assess the relationship between *dxr* phenotypes and GAs, the *dxr* mutant was treated with exogenous GA_3. 7-Day-old homozygous *dxr* seedlings with open cotyledons were transferred onto the MS medium supplied with 10 μM GA_3 and grown for 3 weeks. It is evident that the plants grew higher and faster. The leaves expanded, and leaf petioles grew longer. Most plants could bolt and developed inflorescences with normal flower organs (Figure 8A and 8C). Meanwhile, the trichome initiation defect of *dxr* mutant could be partially rescued (Figure 8B). This result suggests that the phenotypes in the *dxr* mutant may partially result from GA deficiency, and that other metabolites synthesized from the MEP pathway might also be involved in regulating trichome development.

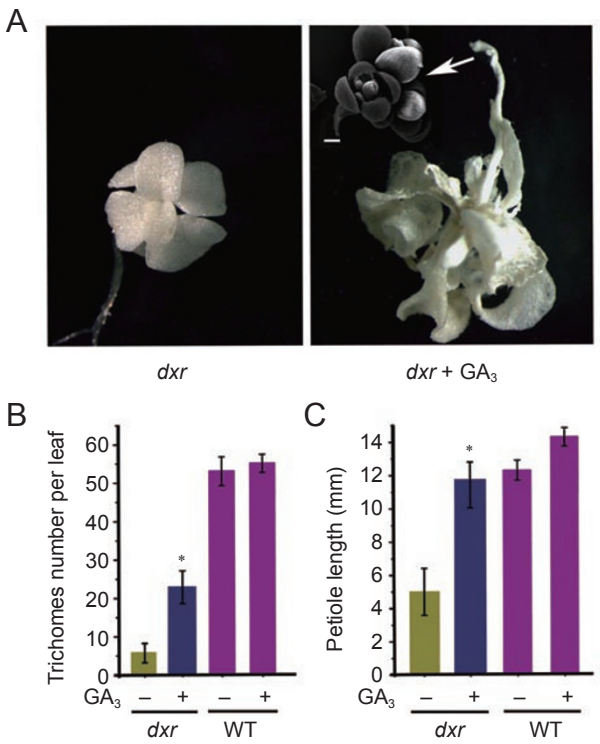

Figure 8 Exogenous application of GA_3 on dxr mutant. **(A)** *dxr* mutant without GA_3 treatment and *dxr* mutant with 10 μM GA_3 treatment. The flower developed from *dxr* mutant treated with 10 μM GA_3 was also shown. Bar = 80 μM. **(B)** Statistical analyses of trichome number on WT and *dxr* leaves with or without GA_3 treatment. WT: 53 ± 3.7 ($n \geq 10$), *dxr*: 5.75 ± 2.5 ($n \geq 10$), dxr (with GA_3 treatment): 22.8 ± 4.3 ($n \geq 8$). **(C)** Measurement of petiole length of *dxr* mutant leaves with or without GA_3 treatment. *dxr*: 5 mm ± 1.4 ($n \geq 10$); *dxr* (with GA_3 treatment): 11.8 mm ± 1.7 ($n \geq 10$). Asterisks mark significant changes.

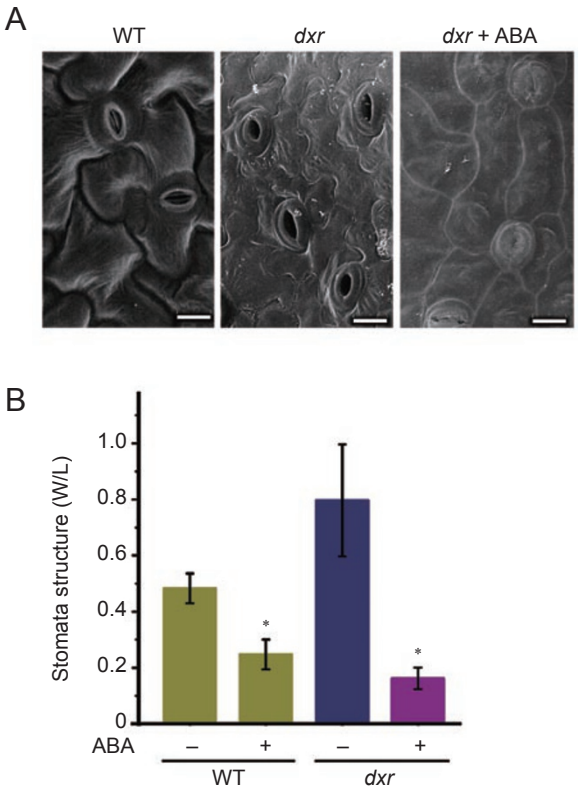

Figure 9 Exogenous application of ABA on *dxr* mutant. **(A)** Stomata structure of WT plants and *dxr* mutant with or without ABA treatment. **(B)** Statistical analyses to the stomata structure (width/length) of WT plants and dxr mutant with or without ABA treatment. WT: 0.48 ± 0.05; *dxr*: 0.83 ± 0.2; *dxr* (with ABA treatment): 0.14 ± 0.04. More than 30 stomatas from at least seven different leaves were measured for each sample. Asterisks mark significant changes.

Exogenous application of ABA could completely rescue the stomata closure phenotype in dxr mutant

ABA, the other important phytohormone synthesized by the MEP pathway, plays a major role in the regulation of stomata opening and closing. In order to find out whether the stomata-closing defects were caused

by a deficiency in ABA, 20-day-old *dxr* seedlings were transferred to the MS medium supplied with 5 μM ABA, and grown for 5 days before they were analyzed for the stomata structure by SEM. The result showed that in the presence of exogenous ABA the stomata closed normally in *dxr* mutants (Figure 9A). This was also revealed by statistical analysis of the corresponding changes of stomata structure (Figure 9B). This result suggests that ABA deficiency is the cause for the stomata-closing defects in the *dxr* mutant.

Discussion

In plants, the MEP pathway provides the five-carbon units, IPP and DMAPP, for the biosynthesis of many important isoprenoids [29]. It has been shown that disturbance to the down-stream steps of MEP-related isoprenoid biosynthetic pathways seriously affects plant development [46].

In this study, with an attempt to completely block the whole MEP pathway, we found that the *dxr* mutant plants displayed severe developmental defects, for instance, abnormal chlorophyll biosynthesis. Like the other albino mutants of the enzymes involved in MEP-related biosynthetic pathways, the *dxr* mutants exhibited an arrest in plastid development at early stages [20, 22, 30, 46-48]. This is consistent with the increased chlorophyll a/b ratio observed in the pale inflorescence tissues, which are more sensitive to light due to the undeveloped plastids [49]. In addition to the albino phenotype, we also found trichome initiation and stomata closure defects as a result of *DXR* disruption. It was previously reported that GAs play important roles in trichome development by regulating trichome-associated genes including *GL1*, *GL3*, and *SPY* [41-45]. As GAs are a class of important products derived from MEP-related isoprenoid biosynthetic pathways, it is reasonable to link *DXR* disruption to the observed trichome developmental defects. However, the regulation of trichome development is complex. The interaction between plant and environmental cues is another important factor that may affect this process [44, 50]. On one hand, the albino phenotype might lead to a hypersensitive response of the *dxr* mutants to environmental stresses. This may help explain why exogenous application of GA_3 can only partially rescue the trichome initiation defect of *dxr*, and why the expression of trichome development regulators changes in the *dxr* mutant. On the other hand, the stomata closure defect in the *dxr* mutants suggests that the biosynthesis of ABA, an important interaction signal molecule between environment and plant [51], is abnormal. It is reasonable to predict that the environmental regulation of trichome development is possibly abnormal in the *dxr* mutant. ABA is also believed to be involved in plant development as an antagonist of GAs. Since gibberellins were shown to be able to interact with jasmonic acid and salicylic acid pathways to regulate trichome development [52], it would be interesting to investigate in the future whether the antagonistic interaction between GAs and ABA also plays a role in trichome development.

The regulation of flux in biosynthetic pathways is an attractive but complicated biological question. To gain more insight into the metabolic flux of the MEP pathway, we monitored the transcript changes in the *dxr* mutants, of those important enzymes involved in the MEP pathway and related isoprenoid biosynthetic pathways. In the albino tissues with reduced *DXR* transcript level, all the examined genes exhibited reduced transcription, which is similar to the gene expression pattern in the *cla1/dxs* and *pds3* mutants [7, 29, 30]. This is an interesting phenomenon, since these three enzymes catalyze different steps in the isoprenoid biosynthetic pathways, i.e., DXR and DXS catalyzing the initial two steps of the MEP pathway, and PDS3 catalyzing a down-stream reaction leading to ABA biosynthesis (Figure 1). In *pds3* mutant, it was suggested that there might be a feedback control of the transcription of enzymes involved in the isoprenoid biosynthetic pathway by the accumulated phytoene, the substrate for the PDS3 enzyme [30]. This feedback control indirectly led to decreased GA biosynthesis, a branch different from the ABA metabolic pathway. From this study, it seems that the expression of down-stream genes in the isoprenoid biosynthetic pathway is also feedback regulated by the insufficiency of initial substrates IPP and DMAPP (Figure 1). In the meantime, the result suggests that transcription of those enzymes involved in plastid isoprenoid biosynthesis is somehow coordinately regulated, leading to the decrease of both ABA and GA biosynthesis in the *dxr* mutant. A more detailed analysis on the mutants of other enzymes involved in the same pathway is needed in the future. As for the *DXR* overexpressing leaves, the increase in *DXR* transcript level did not lead to the accumulation of photosynthetic pigments. There are at least two possibilities. One is post-transcriptional regulation of DXR, such as translational modulation [19, 53]. In *Arabidopsis*, HMGR, a critical enzyme involved in the MVA pathway, has even more complicated regulation mechanisms [26, 54-57]. The other possibility is that DXR might not be a determinant enzyme in the MEP pathway. In this pathway, DXS has been identified to catalyze the first step, the key step of the MEP pathway, in Arabidopsis [22, 47, 58]. *DXS* was also found to share a similar expression pattern with *DXR*, and both *DXS* and *DXR* null mutants displayed an

albino phenotype [7, 19, 22, 47]. Many studies on comparisons between DXR and DXS have also been carried out [7, 19]. Possibly, for those non-determinant enzymes such as DXR, their expression levels are normally more than needed, and metabolic changes will only be triggered after the changes of the enzymes reach a certain threshold.

Crosstalk between the MEP and MVA pathways is an interesting topic. It is generally believed that the chemical flux is mainly from MEP to the MVA pathway [7, 29, 59]. In our study, without the functional MEP pathway, plants can still survive for a long period until the bolting stage. There are two possibilities. One possibility is that the chemical storage in homozygous mutant seeds is sufficient to support plant growth and development. The other possibility is that chemical flux from the MVA pathway is able to fulfil part of the biosynthesis requirement of the MEP pathway. As reported previously, sucrose can modulate the carbon flux through the MEP pathway, possibly either as a carbon source or as an energy indicator [53, 60]. Taking into consideration that, without sucrose, the *dxr* null mutant plants are arrested at an early developmental stage, but with sucrose the mutant can proceed with the basic differentiation program and grow for more than 40 days, in which GAs, ABA or other important carotenoids are necessarily involved [61], the second possibility seems more likely. As carbon flux through the MEP pathway is completely blocked in the *dxr* mutant, it would be interesting to investigate the potential important role of sucrose in promoting the carbon flow from MVA pathway to the MEP pathway, facilitating the supply of the necessary amount of GAs or ABA.

It was previously reported that the MVA pathway plays a more important role than the MEP pathway during reproductive development in *Arabidopsis* [62, 63]. Another interesting phenomenon from our study is that the heterozygous *dxr* mutant plants set normal homozygous seeds, suggesting that, without the MEP pathway, the gametophytes, embryo sac or later-developed homozygous embryo can develop normally, consistent with the previous reports. In other words, the possible crosstalk and flux between the MVA pathway and the MEP pathway are sufficient to fulfil the chemical requirement in germ cells and embryo development. As the main flux is shown to be normally from the MEP pathway to the MVA pathway [7, 29, 59], we suspect that the direction of the main flux may change at different developmental stages or under certain conditions. Due to the technique limitation for chemical detection *in planta*, it will be a great challenge to clarify the real-time image of the crosstalk flux in plants in the future.

In summary, by characterizing the phenotypes of *dxr* mutant and two *DXR* transgenic co-suppression lines, we found that complete blockage of the MEP pathway in *dxr* mutant results in typical carotenoid-deficiency phenotypes, including abnormal chloroplast and trichome development, possibly due to significant precursor deficiency for GAs and ABA biosynthesis. Detailed analysis of the *dxr* mutant provides evidence that the plastidial MEP biosynthetic pathway plays an essential role in plant development by regulating the isoprenoid biosynthetic pathway.

Materials and Methods

Plant material and growth conditions

Arabidopsis thaliana, ecotype Columbia-0, was used. The seeds of *dxr* mutant were requested from GABI-Kat. Plants were grown on Murashige and Skoog plates (GIBCO/BRL, Cleveland, OH, USA), pH adjusted to 5.7 with 1 M of KOH, containing 0.8% (w/v) phytoagar and 1% sucrose, or in soil in the greenhouse under long-day conditions (16-h-light/8-h-dark cycle) at 22 °C ± 1 °C. For GAs or ABA treatment, 10 μM of GA_3 or 5 μM of ABA was applied to the MS medium in the plate or conical flask.

DXR cloning, vector construction and over-expression in Arabidopsis

The PCR product of the *DXR* full-length coding region was cloned into pBlueScript SK(+/–) (Stratagene, La Jolla, CA, USA) and sequenced. The *DXR* fragment cut by *Bam*HI and *Sal*I restriction enzymes was then constructed into the plant expression vector, pQG110, driven by a Cauliflower Mosaic Virus (CaMV) 35S promoter. The construct was transformed into *Agrobacterium tumefaciens* GV3101/pMP90. *Arabidopsis* plants grown in soil for one and a half months were transformed using the floral dip method [64]. Transgenic plants screening was carried out as previously reported [65]. Their identities were later confirmed by PCR using the *DXR*-specific primers: 5′-ATG ATG ACA TTA AAC TCA CTA TCT CCA G-3′ and 5′-TCA TGC ATG AAC TGG CC TAG CAC CA-3′. Seeds were collected at maturity and stored at 4 °C.

RNA extraction and reverse transcription

Total RNA from the frozen material was extracted using TRIzol Reagent. To eliminate the contamination of genomic DNA, total RNA was then treated with RNase-free DNase (Takara). In all, 5 μg of total RNA was reverse-transcribed using the SuperscriptΠ RT Kit (Invitrogen, Carlsbad, CA, USA), in a reaction of 20 μl. The cDNA was diluted 50 times and later used as the template for RT-PCR [66].

Quantitative real-time RT-PCR

The PCR amplification was performed on a MJ Research thermocycler, using a DyNAmo SYBR Green qPCR kit from Finnzymes (distributed by MJ research, incorporated; F-400L). Each reaction was carried out on a 1 μl diluted cDNA sample, in a total reaction system of 10 μl. The procedure of the reaction was set according to the manufacturer's protocol. To check the specificity of amplification, the melting curve of the PCR products was determined. The expression levels of different genes were standardized to the constitutive expression level of *Tubulin2*.

In one real-time PCR experiment, at least three values were produced for each sample, as previously reported [67]. The relative expression level of each gene, corresponding to the expression level of *Tubulin2*, was calculated using the $2^{-\Delta\Delta t}$ method [68]. The primers used for the quantitative real-time PCR are listed in Supplementary information, Table S1.

Chlorophyll and carotenoid analysis

Chlorophyll and carotenoids were extracted from *A. thaliana* leaves and inflorescence using a method modified by Gitelson *et al.* [69]. Briefly, 4th~7th rosette leaves harvested from 3-week-old plants or the inflorescences from 6-week-old plants were put into a pre-chilled tube, and ground for 3 min in 1 ml extraction buffer (85% acetone: Tris-HCl [1%, w/v]). After the pigments were completely extracted by the buffer, an additional 1 ml extraction buffer was used to wash the pestle. All extraction solutions were combined and debris was removed by centrifugation. A volume of 1 ml of the supernatant was diluted to 3 ml final solution. The light absorbance of the final solution at 663, 647 and 470 nm was measured. The concentrations of carotenoids and chlorophyll were calculated as described [70].

Transmission electron microscope

TEM was conducted following the procedure described by Hsieh and Goodman, with a few modifications [30, 60]. The seedling samples were fixed in 4% glutaraldehyde overnight, and post-fixed with 1% osmium tetroxide for 30 min. The fixed samples were dehydrated through a series of alcohol solutions and embedded in Spurr resin. The ultra-thin sections were cut on a Reichert Ultracut-S (Leica Microsystems, Bannockburn, IL, USA) and stained with uranyl acetate and lead citrate before being viewed with a TEM (Hitachi, Tokyo, Japan).

Scanning electron microscope

SEM analysis was performed as described previously [71]. The samples were viewed using a SEM.

Acknowledgments

This work was supported by the National Natural Science Foundation of China (NSFC Grant 90717003 to L-J Qu).

References

1 Chappell J. The biochemistry and molecular biology of isoprenoid metabolism. *Plant Physiol* 1995; **107**:1-6.
2 Chappell J. The genetics and molecular genetics of terpene and sterol origami. *Curr Opin Plant Biol* 2002; **5**:151-157.
3 McGarvey DJ, Croteau R. Terpenoid metabolism. *Plant Cell* 1995; **7**:1015-1026.
4 Eisenreich W, Schwarz M, Cartayrade A, Arigoni D, Zenk MH, Bacher A. The deoxy-xylulose phosphate pathway of the terpenoid biosynthesis in plants and microorganisms. *Chem Biol* 1998; **5**:R221-R233.
5 Lichtenthaler HK. The 1-deoxy-D-xylulose-5-phosphate pathway of isoprenoid biosynthesis in plants. *Annu Rev Plant Physiol Plant Mol Biol* 1999; **50**:47-65.
6 Rohmer M. The discovery of a mevalonate-independent pathway for isoprenoid biosynthesis in bacteria, algae and higher plants. *Nat Prod Rep* 1999; **16**:565-574.
7 Laule O, Fürholz A, Chang HS, *et al.* Crosstalk between cytosolic and plastidial pathways of isoprenoid biosynthesis in *Arabidopsis thaliana*. *Proc Natl Acad Sci USA* 2003; **100**:6866-6871.
8 Arigoni D, Sagner S, Latzel C, Eisenreich W, Bacher A, Zenk MH. Terpenoids biosynthesis from 1-deoxy-D-xylulose in higher plants by intramolecular skeletal rearrangement. *Proc Natl Acad Sci USA* 1997; **94**:10600-10605.
9 Eisenreich W, Rohdich F, Bacher A. Deoxyxylulose phosphate pathway to terpenoids. *Trends Plant Sci* 2001; **6**:78-84.
10 Rohmer M, Knani M, Simonin P, Sutter B, Sahm H. Isoprenoid biosynthesis in bacteria: a novel pathway for the early steps leading to isopentenyl diphosphate. *Biochem J* 1993; **295**:517-524.
11 Rohmer M, Seemann M, Horbach S, Bringer-Meyer S, Sahm H. Glyceraldehyde 3-phosphate and pyruvate as precursors of isoprenic units in an alternative non-mevalonate pathway for terpenoid biosynthesis. *J Am Chem Soc* 1996; **118**:2564-2566.
12 Sprenger GA, Schörken U, Wiegert T, *et al.* Identification of a thiamin-dependent synthase in *Escherichia coli* required for the formation of the 1-deoxy-D-xylulose 5-phosphate precursor to isoprenoids, thiamine, and pyridoxol. *Proc Natl Acad Sci USA* 1997; **94**:12857-12862.
13 Lois LM, Campos N, Putra SR, Danielsen K, Rohmer M, Boronat A. Cloning and characterization of a gene from *Escherichia coli* encoding a transketolase-like enzyme that catalyzes the synthesis of D-1-deoxyxylulose 5-phosphate, a common precursor for isoprenoid, thiamin, and pyridoxol biosynthesis. *Proc Natl Acad Sci USA* 1998; **95**:2105-2110.
14 Takahashi S, Kuzuyama T, Watanabe H, Seto H. A 1-deoxy-D-xylulose 5-phosphate reductoisomerase catalyzing the formation of 2-C-methyl-D-erythritol 4-phosphate in an alternative non-mevalonate pathway for terpenoid biosynthesis. *Proc Natl Acad Sci USA* 1998; **95**:9879-9884.
15 Hecht S, Eisenreich W, Adam P, *et al.* Studies on the non-mevalonate pathway to terpenes: the role of the GcpE (IspG) protein. *Proc Natl Acad Sci USA* 2001; **98**:14837-14842.
16 Hintz M, Reichenberg A, Altincicek B, *et al.* Identification of (*E*)-4-hydroxy-3-methyl-but-2-enyl pyrophosphate as a major activator for human γδ T cells in *Escherichia coli. FEBS Lett* 2001; **509**:317-322.
17 Julliard JH, Douce R. Biosynthesis of the thiazole moiety of thiamin (vitamin B1) in higher plant chloroplasts. *Proc Natl Acad Sci USA* 1991; **88**:2042-2045.
18 Fitzpatrick TB, Amrhein N, Kappes B, Macheroux P, Tews I, Raschle T. Two independent routs of *de novo* Vitamin B_6 biosynthesis: not that different at all. *Biochem J* 2007; **407**:1-13.
19 Carretero-Paulet L, Cunillera N, Rodrguez-Concepcio M, Ferrer A, Boronat A. Expression and molecular analysis of the *Arabidopsis DXR* gene encoding 1-deoxy-D-xylulose 5-phosphate reductoisomerase, the first committed enzyme of the 2-C-methyl-D-erythritol 4-phosphate pathway. *Plant Physiol* 2002; **129**:1581-1591.
20 Carretero-Paulet L, Cairó A, Botella-Pavía P, *et al.* Enhanced flux through the methylerythritol 4-phosphate pathway in *Arabidopsis* plants over-expressing deoxyxylulose 5-phosphate reductoisomerase. *Plant Mol Biol* 2006; **62**:683-695.
21 Mahmoud SS, Croteau RB. Metabolic engineering of essen-

tial oil yield and composition in mint by altering expression of deoxyxylulose phosphate reductoisomerase and menthofuran synthase. *Proc Natl Acad Sci USA* 2001; **98**:8915-8920.
22 Estévez JM, Cantero A, Reindl A, Reichler S, León P. 1-deoxy-D-xylulose-5-phosphate synthase, a limiting enzyme for plastidic isoprenoid biosynthesis in plants. *J Biol Chem* 2001; **276**:22901-22909.
23 Zeidler J, Schwender J, Müller C, *et al*. Inhibition of the non-mevalonate 1-deoxy-D-xylulose-5-phosphate pathway of plant isoprenoid biosynthesis by fosmidomycin. *Z Naturforsch* 1998; **53**:980-986.
24 Rodríguez-Concepción M, Ahumada I, Diez-Juez E, *et al*. 1-deoxy-D-xylulose 5-phosphate reductoisomerase and plastid isoprenoid biosynthesis during tomato fruit ripening. *Plant J* 2001; **27**:213-222.
25 Okada K, Kawaide H, Kuzuyama T, Seto H, Curtis I, Kamiya Y. Antisense and chemical suppression of the non-mevalonate pathway affects ent-kaurene biosynthesis in *Arabidopsis*. *Planta* 2002; **215**:339-344.
26 Rodríguez-Concepción M, Martínez-García JF, González V, Phillips MA, Ferrer A, Boronat A. Distinct light-mediated pathways regulate the biosynthesis and exchange of isoprenoid precursors during *Arabidopsis* seedling development. *Plant Cell* 2004; **16**:144-156.
27 Budziszewski GJ, Lewis SP, Glover LW, *et al. Arabidopsis* genes essential for seedling viability: isolation of insertional mutants and molecular cloning. *Genetics* 2001; **159**:1765-1778.
28 Sun TP, Kamiya Y. The *Arabidopsis* GA1 locus encodes the cyclase ent-kaurence synthetase A of gibberellin biosynthesis. *Plant Cell* 1994; **6**:1509-1518.
29 Rodríguez-Concepción M. Early steps in isoprenoids biosynthesis: multilevel regulation of the supply of common precursors in plant cells. *Phytochemistry Rev* 2006; **5**:1-15.
30 Qin G, Gu H, Ma L, *et al.* Disruption of *phytoene desaturase* gene results in albino and dwarf phenotypes in *Arabidopsis* by impairing chlorophyll, carotenoid, and gibberellin biosynthesis. *Cell Res* 2007; **17**:471-482.
31 Botella-Pavía P, Besumbes Ó, Phillips MA, Carretero-Paulet L, Boronat A, Rodríguez-Concepción M. Regulation of carotenoid biosynthesis in plants: evidence for a key role of hydroxymethylbutenyl diphosphate reductase in controlling the supply of plastidial isoprenoid precursors. *Plant J* 2004; **40**:188-199.
32 Page JE, Hause G, Raschke M, *et al.* Functional analysis of the final steps of the 1-deoxy-D-xylulose 5-phosphate (DXP) pathway to isoprenoids in plants using virus-induced gene silencing. *Plant Physiol* 2004; **134**:1401-1413.
33 Barta C, Loreto F. The relationship between the methylerythriol phosphate pathway leading to emission of volatile isoprenoids and abscisic acid content in leaves. *Plant Physiol* 2006; **141**:1676-1683.
34 Dong H, Deng Y, Mu J, *et al.* The *Arabidopsis Spontaneous Cell Death1* gene, encoding a ζ-carotene desaturase essential for carotenoid biosynthesis, is involved in chloroplast development, photoprotection and retrograde signaling. *Cell Res* 2007; **17**:458-470.
35 Li Y, Rosso MG, Strizhov N, Viehoever P, Weisshaar B. GABI-Kat SimpleSearch: a flanking sequence tag (FST) database for the identification of T-DNA insertion mutants in *Arabidopsis thaliana*. *Bioinformatics* 2003; **19**:1441-1442.
36 Oppenheimer DG, Herman PL, Sivakumaran S, Esch J, Marks MD. A *myb* gene required for leaf trichome differentiation in *Arabidopsis* is expressed in stipules. *Cell* 1991; **67**:483-493.
37 Walker AR, Davison PA, Bolognesi-Winfield AC, *et al.* The TTG1 (transparent testa, glabra1) locus which regulates trichome differentiation and anthocyanin biosynthesis in *Arabidopsis* encodes a WD40-repeat protein. *Plant Cell* 1999; **11**:1337-1350.
38 Payne CT, Zhang F, Lloyd AM. GL3 encodes a bHLH protein that regulates trichome development in *Arabidopsis* through interaction with GL1 and TTG1. *Genetics* 2000; **156**:1349-1362.
39 Wang S, Wang JW, Yu N, *et al.* Control of plant trichome development by a cotton fiber MYB gene. *Plant Cell* 2004; **16**:2323-2334.
40 Schellmann S, Hülskamp, M. Epidermal differentiation: trichomes in *Arabidopsis* as a model system. *Int J Dev Biol* 2005; **49**:579-584.
41 Gan Y, Yu H, Peng J, Broun P. Genetic and molecular regulation by DELLA proteins of trichome development in *Arabidopsis*. *Plant Physiol* 2007; **145**:1031-1042.
42 Silverstone AL, Tseng T, Swains SM, *et al.* Functional analysis of SPINDLY in gibberellin signaling in *Arabidopsis*. *Plant Physiol* 2007; **143**:987-1000.
43 Perazza D, Vachon G, Herzog M. Gibberellins promote trichome formation by up-regulating GLABROUS1 in *Arabidopsis*. *Plant Physiol* 1998; **117**:375-383.
44 Hülskamp M. Plant trichomes: a model for cell differentiation. *Nat Rev Mol Cell Biol* 2004; **5**:471-480.
45 Ishida T, Kurata T, Okada K, Wada T. A genetic regulatory network in the development of trichomes and root hairs. *Annu Rev Plant Biol* 2008; **59**:365-386.
46 Bouvier F, Rahier A, Camara B. Biogenesis, molecular regulation and function of plant isoprenoids. *Prog Lipid Res* 2005; **44**:357-429.
47 Estévez JM, Cantero A, Romero C, *et al.* Analysis of the expression of *CLA1,* a gene that encodes the 1-deoxyxylulose 5-phosphate synthase of the 2-C-methyl-D-erythritol-4-phospate pathway in *Arabidopsis*. *Plant Physiol* 2000; **124**:95-103.
48 Hsieh MH, Chang CY, Hsu SJ, Chen JJ. Chloroplast localization of methylerythritol 4-phosphate pathway enzymes and regulation of mitochondrial genes in *ispD* and *ispE* albino mutants in *Arabidopsis*. *Plant Mol Biol* 2008; **66**:663-673.
49 Reger BJ, Krauss RW. The photosynthetic response to a shift in the chlorophyll *a* to chlorophyll *b* ratio of *Chlorella*. *Plant Physiol* 1970; **46**:568-575.
50 Gianfaga TJ, Carter CD, Sacalis JN. Temperature and photoperiod influence trichome density and sesquiterpene content of *Lycopersicon hirsutum f. hirsutum. Plant Physiol* 1992; **100**:1403-1405.
51 Buchanan BB, Gruissem W, Jones RL. *Biochemistry and Molecular Biology of Plants*. Rockville, MD: American Society of Plant Physiologists, 2000.
52 Traw MB, Bergelson J. Interaction effects of jasmonic acid, salicylic acid and gibberellin on induction of trichomes in *Arabidopsis*. *Plant Physiol* 2003; **133**:1-9.

53 Cordoba E, Salmi M, León P. Unravelling the regulatory mechanisms that modulate the MEP pathway in higher plants. *J Exp Bot* 2009; **60**:2933-2943.
54 Dale S, Arro M, Becerra B, *et al.* Bacterial expression of the catalytic domain of 3-hydroxy-3-methylglutaryl-CoA reductase (isoform HMGR1) from *Arabidopsis thaliana*, and its inactivation by phosphorylation at Ser577 by *Brassica oleracea* 3-hydroxy-3-methylglutaryl-CoA reductase kinase. *Eur J Biochem* 1995; **233**:506-513.
55 Learned RM. Light suppresses 3-hydroxy-3-methylglutaryl-CoA reductase gene expression in *Arabidopsis thaliana*. *Plant Physiol* 1996; **110**:645-655.
56 Newman JD, Chappell J. Isoprenoid biosynthesis in plants: carbon partitioning within the cytoplasmic pathway. In: Parish EJ, Nes WD, eds. *Biochemistry and Function of Sterols*. CRC Press: Boca Raton, FL, 1997:123-134.
57 Kobayashi K, Suzuki M, Tang J, *et al.* LOVASTATIN INSENSITIVE 1, a novel pentatricopeptide repeat protein, is a potential regulatory factor of isoprenoid biosynthesis in *Arabidopsis*. *Plant Cell Physiol* 2007; **48**:322-331.
58 Mandel MA, Feldmann KA, Herrera-Estrella L, Rocha-Sosa M, León P. *CLA1*, a novel gene required for chloroplast development, is highly conserved in evolution. *Plant J* 1996; **9**:649-658.
59 Bick JA, Lange BM. Metabolic cross talk between cytosolic and plastidial pathways of isoprenoids biosynthesis: unidirectional transport of intermediates across the chloroplast envelope membrane. *Arch Biochem Biophys* 2003; **451**:146-154.
60 Hsieh MH, Goodman HM. The *Arabidopsis* IspH homolog is involved in the plastid non-mevalonate pathway of isoprenoid biosynthesis. *Plant Physiol* 2005; **138**:641-653.
61 Ogas J, Cheng JC, Sung ZR, Somerville C. Cellular differentiation regulated by Gibberellin in the *Arabidopsis thaliana pickle* mutant. *Science* 1997; **277**:91-94.
62 Clouse SD. *Arabidopsis* mutants reveal multiple roles for sterols in plant development. *Plant Cell* 2002; **14**:1995-2000.
63 Suzuki M, Nakagawa S, Kamide Y, *et al.* Complete blockage of the mevalonate pathway results in male gametophyte lethality. *J Exp Bot* 2009; **60**:2055-2064.
64 Clough SJ, Bent AF. Floral dip: A simplified method for *Agrobacterium*-mediated transformation of *Arabidopsis thaliana*. *Plant J* 1998; **16**:735-743.
65 Qin G, Gu H, Zhao Y, *et al.* Indole-3-acetic acid carboxyl methyltransferase regulates *Arabidopsis* leaf development. *Plant Cell* 2005; **17**:2693-2704.
66 Liu J, Zhang Y, Qin G, *et al.* Targeted degradation of the cyclin-dependent kinase inhibitor ICK4/KRP6 by RING-type E3 ligases is essential for mitotic cell cycle progression during *Arabidopsis* gametogenesis. *Plant Cell* 2008; **20**:1538-1554.
67 Guo L, Wang Z, Lin H, *et al.* Expression and functional analysis of rice plasma-membrane intrinsic protein gene family. *Cell Res* 2006; **16**:277-286.
68 Livak KJ, Schmittgen TD. Analysis of relative gene expression data using real-time quantitative PCR and the $2^{-\Delta\Delta t}$ method. *Methods* 2001; **25**:402-408.
69 Gitelson AA, Gritz Y, Merzlyak MN. Relationships between leaf chlorophyll content and spectral reflectance and algorithms for non-destructive chlorophyll assessment in higher plant leaves. *J Plant Physiol* 2003; **160**:271-282.
70 Lichtenthaler HK. Chlorophyll florescence signature of leave the autumnal chlorophyll breakdown. *J Plant Physiol* 1987; **131**:101-110.
71 Yadegari R, De Paiva GR, Laux T, *et al.* Cell differentiation and morphogenesis are uncoupled in *Arabidopsis raspberry* embryos. *Plant Cell* 1994; **6**:1713-1729.

(**Supplementary information** is linked to the online version of the paper on the *Cell Research* website.)